ON THE X-RAY EMISSION FROM THE RADIO SOURCE SGR A*

R. F. Coker
Los Alamos National Laboratory
T087, LANL, Los Alamos, NM 87545, U.S.A.
ROBC@LANL.GOV
J. M. Pittard
School of Physics & Astronomy, University of Leeds
Woodhouse Lane, Leeds, LS2 9JT, UK
JMP@AST.LEEDS.AC.UK

Abstract

Recent infrared observations of the Galactic center have permitted the estimation of orbital parameters for the eight O stars closest to the compact, non-thermal radio source, Sagittarius A* (Sgr A*). The emission of Sgr A* is thought to be due to the accretion of gas down the potential well of a 3×10^6 solar mass black hole at the dynamical heart of the Milky Way. The O stars are located within 0.03 parsec of Sgr A* and are likely to have significant stellar winds. Since they are deep within the potential well of a black hole, much of their winds are gravitationally bound. These hot winds may be piling up and emitting significantly in the X-rays. Thus it is possible that the emission from the recently detected compact *Chandra* source may, at least in part, be due to the winds of these O stars rather than the hot gas close to the event horizon of the black hole. This has serious implications for applicable black hole accretion models. From preliminary three dimensional numerical simulations which treat the eight O stars as mass and energy sources moving on individual orbits, we have constructed simulated X-ray images. We present these images and discuss their impact on accretion models for Sgr A*.

1 Introduction

Sgr A* is a strong, compact radio source located at the dynamical center of the Galaxy. The radio emission is thought to arise from gas falling down the steep potential well of a 3×10^6 $M_\odot$ black hole (Melia & Falcke, 2001). However, Sgr A* has not been definitively detected at other wavelengths due to the large extinction between us and the Galactic center (GC). It has been expected that there would be significant X-ray emission due to thermal bremsstrahlung and upscattered magnetic bremsstrahlung radio emission (Yuan, Markoff & Falcke, 2002). Recent *Chandra* X-ray images do indeed show a point source within the $\sim 1''$ astrometric error box of Sgr A*. The point source has been seen to flare and is surrounded by $\sim 10''$ of diffuse emission in the 2–10 keV *Chandra* band (Baganoff et al., 2001, 2003). The details of the point source have been used to constrain models of the gas accretion onto Sgr A* (Falcke, Körding & Markoff, 2004).

2 Another possible source of X-rays

There are at least eight late-type O stars located within $\sim 1''$ of Sgr A* in projection (at 8 kpc, the distance of the GC, $1'' \simeq 0.04$ pc). From infrared Keck observations, these stars now have measured orbital parameters (Ghez et al., 2004) and although some have large error bars, they are very likely to be orbiting a point mass of $\sim 3.5\times10^6$ $M_\odot$. One star, with an orbital period of ~ 15 years, has been detected with an orbital velocity of more than 5000 km s^{-1}; within a few decades it will serve as a unique test of general relativity due to the precession of its orbit (Weinberg, Milosavljevic & Ghez, 2004). It is worth noting that some of the stars' orbits are highly elliptical, suggesting recent ejection due to a close approach to the black hole. Clearly, the strong, hot winds of these stars will contribute to the X-ray flux seen by *Chandra*. We ignore here the winds from two dozen Wolf-Rayet and early O stars in the IRS16 and IRS13 clusters (Geballe, Krisciunas, Bailey & Wade, 1991); these stars are more than 10 times further away from Sgr A* and are likely to contribute substantially to the more extended *Chan-*

dra X-ray emission (Rockefeller, Fryer, Melia & Warren, 2004). Since there are so many stars in such a small volume, strong wind collisions and shocks will dissipate sufficient kinetic energy to result in significant X-ray emission. This then leads us to the question: how much of the observed point-source X-ray flux is from close to the event horizon of the black hole and how much is extended emission due to colliding stellar winds?

3 Numerical approach and included physics

In order to make the simulations run in a practical amount of time, we use RAGE, a three-dimensional Eulerian continuous adaptive mesh refinement (CAMR) code with 2nd order Godunuv hydrodynamics and a Riemann solver (Baltrusaitis et al., 1996). By determining mesh refinement on a cell by cell basis every time step, CAMR uses high resolution only where it is required. For these initial simulations, we use a finest resolution of 1×10^{15} cm. We treat each one of the eight O stars as a moving mass and energy source in a three-dimensional Cartesian hydrodynamics simulation. For simplicity, we assume that all of the eight stars are identical giant O8 stars, although at least one is probably a dwarf (Ghez et al., 2004). We pick low-end conservative mass and energy injection rates for O8 III stars. Although mass loss rates for O8 III stars can be more than an order of magnitude larger (Krtička & Kubát, 2004), we choose a mass injection rate, $\dot{\mathrm{M}} = 2.5\times10^{-7}\ M_\odot\ \mathrm{yr}^{-1}$ and an energy injection rate, $\dot{\mathrm{L}} = 81\ L_\odot$ (Garmany & Conti, 1984). This results in a terminal wind velocity of $\sim 2200\ \mathrm{km\ s}^{-1}$. For details on this method of mass injection for colliding stellar winds, see Pittard & Stevens (1997) and Strickland & Stevens (1998). The injection diameter for each star is 5×10^{15} cm or five cells. Assuming collisional ionization equilibrium and solar abundances for simplicity, we perform a radiative transfer calculation to produce synthetic X-ray images, spectra, and luminosities at various simulation times.

We include not only the gravitational potential from a $3.5\times10^6\ M_\odot$ point mass but also that from the underlying (and unseen) stellar cluster. Since the mass accretion rate across the event horizon is thought to be small (Yuan, Quataert & Narayan, 2003) compared to the total mass being injected into the grid, we do not remove any material near the black hole. We assume the gas is optically thin so that we can include radiative cooling

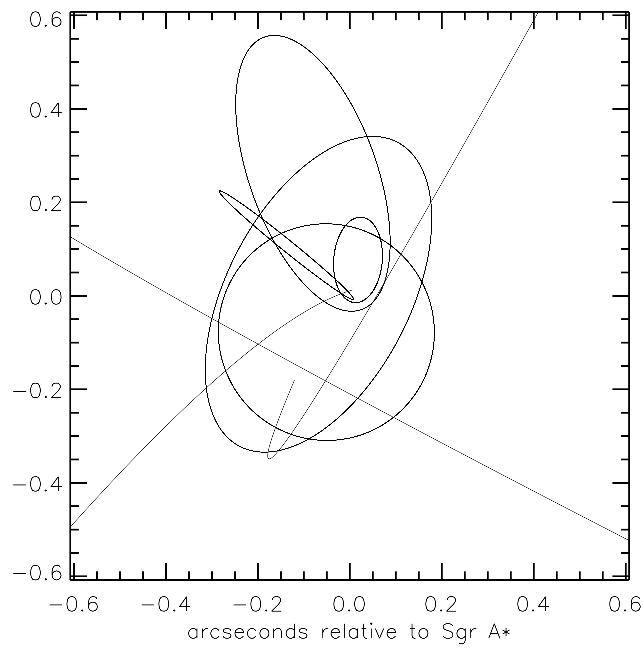

Figure 1: The projected orbits of the eight O stars for the volume of the simulation (1.2″ on a side). The start of the orbits is at time zero and corresponds to 1989. For some unknown reason, the orbit of S0-3 (the star that cuts completely across the field of view) does not match that plotted in Ghez et al. (2004), Fig. 2

as a simple energy sink. We use the thermal plasma code MEKAL (Mewe, Gronenschild & van den Oord, 1985), as distributed in `XSPEC`, to calculate the cooling rates. We solve for the location and velocity of each star at each time step and inject the appropriate mass and thermal energy with a momentum that matches the stellar velocity around Sgr A*. That is, the terminal velocity of each wind on the grid is the vector sum of the star velocity plus the wind velocity that arises due to the pressure gradient. We use outflow boundary conditions so as to permit unbound gas to escape the volume of solution. The projected orbits of the eight O8 III stars are shown in Fig. 1. Three stars have open orbits, since their periods ($> 10^3$ years) are longer than the length of the simulations. Nonetheless, if required, these stars are allowed to enter and leave the grid. Although there is a slight bias in their apoapses (Ghez et al., 2004), the eight stars do not define a clear, constant angular momentum vector, so it is interesting that the black hole is inferred to have a very large angular momentum (Aschenbach, Grosso, Porquet & Predehl, 2004). Although collisions are not included in these simulations, the eight O8 III stars are close enough to each other at times that stellar encounters may be sig-

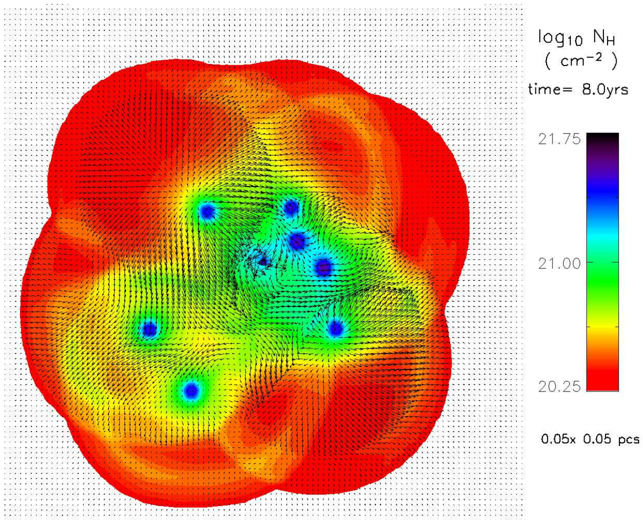

Figure 2: The column density along the line of sight eight years into the simulation. Wind-wind shocks and the gas pile up at Sgr A* can be seen. One star is not yet on the grid at this time.

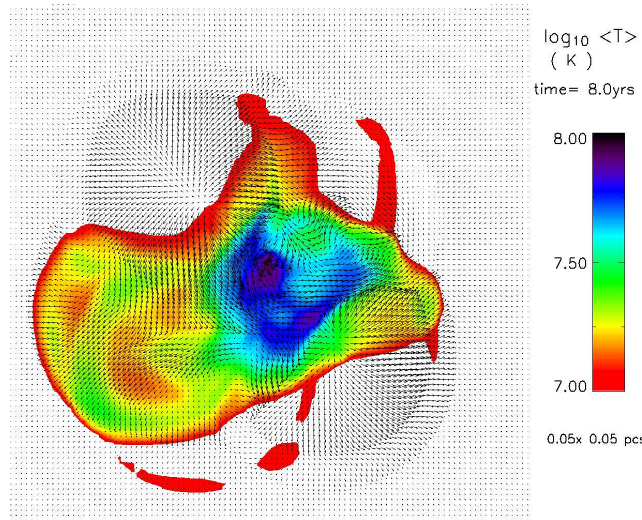

Figure 3: The spatially averaged temperature along the line of sight eight years into the simulation. A hot cavity surrounding Sgr A* can be seen. Note that blue is hot and red is cold.

nificant. The interstellar medium is taken to be a γ = 5/3 gas with n = 10 cm^{-3} and T = 10^4 K. The injected wind is also assumed to be a γ = 5/3 gas with a mean molecular mass of μ = 0.6.

4 Results

4.1 Early time results

In Fig. 2 we show the column density along the line of sight after eight years of simulation time. At this time the winds have not yet filled the volume of solution. Also, the stars have not yet moved very far so that individual wind blown bubbles can still be seen. The velocity, with the largest vectors corresponding to 1000 km s^{-1}, in the xy plane at z = 0 is overlaid on this and following figures. Two stars are nearly in the z = 0 plane at this time and their winds are nearly freely flowing into the interstellar medium; the inner and outer shocks of their winds can be seen in the upper left and lower right of Fig. 2. In Fig. 3 we show the average temperature along the line of sight at the same point in time. Some of the shocks of the wind bubbles can be seen, but the hot bubble around Sgr A* is clearly dominant at high temperatures. Of course, after only eight years, the simulation is far from any equilibrium.

4.2 Later time results

It takes $\sim$ 25 years for the O star winds to fill the central $(1'')^3$ of the Galaxy. As more gas enters the volume, the average column density increases and gas continues to pile up near the black hole. However, the gas-fill is still patchy at 25 years and the calculation has still not converged since the central stars have completed approximately only a single orbit. Thus, the simulation was continued for more than 500 years; at this point the gas density and temperature surrounding Sgr A* has saturated due to the high temperature of the compressed gas and periodic purging by stars passing close to the black hole. By 500 years, the volume around Sgr A* dominates the column density and individual wind blown bubbles are no longer clearly seen (Fig. 4).

We calculate X-ray emission (using MEKAL) and absorption (using CLOUDY, Ferland, 2000) coefficients for each cell at 569 years. Then we use a ray-tracing program to solve the radiation-transfer equation along the line of sight to produce a synthetic 2–10 keV X-ray image and thus estimate the X-ray photon index, luminosity, and spectrum. In Fig. 5 we show the resulting intrinsic and absorbed spectrum at 569 years. Since the gas in the volume of solution is hot, there is very little intrinsic X-ray absorption; rather, the absorption is dominated by the large exterior GC column of $\sim$ 10^{23} cm^{-2}, which heavily absorbs X-ray emis-

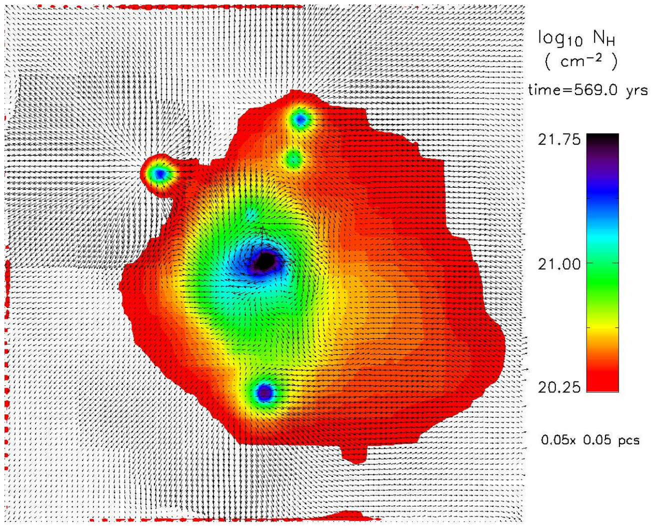

Figure 4: The column density at 569 years. Sgr A* dominates the column. At the edges of the volume, the effects of imperfect outflow boundary conditions can be seen.

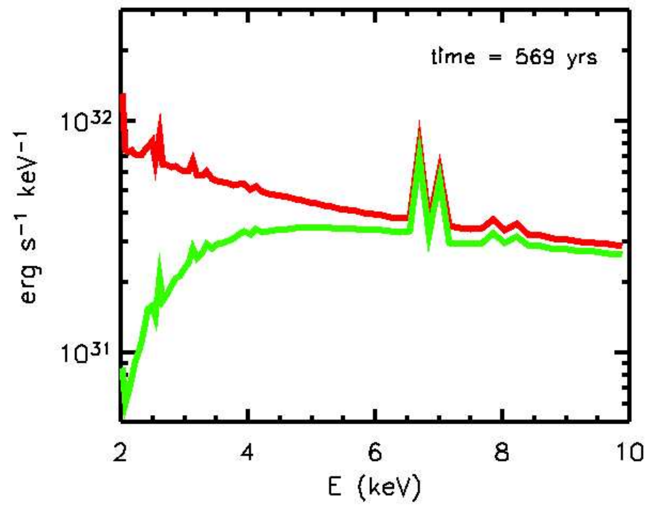

Figure 5: The predicted 2–10 keV X-ray intrinsic (red) and absorbed (green) spectra for the gas distribution shown in Fig. 4. The column toward the GC is taken to be 10^{23} cm^{-2}. To compare to the results of Baganoff et al. (2003), these results need to be convolved with the detector response.

sion below $\sim$ 2 keV. The intrinsic 2–10 keV luminosity is 3.7×10^{32} erg s^{-1} while the absorbed luminosity is 2.4×10^{32} erg s^{-1} and the photon index is $\sim$ 1.6. In Fig. 6 we show the synthetic X-ray image. Since we inject the wind material with its kinetic luminosity in thermal form, some of the stars can be seen in Fig. 6; however, Sgr A* still dominates the X-ray emission. The emission from near Sgr A* is extended on the order of $\sim 0.1''$ or $\sim 10^4 R_s$, where R_s = 2GM/c^2 is the Schwarzschild radius of a black hole of mass M.

5 Discussion and summary

From *Chandra* observations, the estimated intrinsic 2–10 keV luminosity of Sgr A* is 2.4×10^{33} erg s^{-1}. Assuming a power-law model, the observed photon index is between 1.8 and 4.0 with a best fit value of 2.7 (Baganoff et al., 2003). Initial three-dimensional simulations of eight orbiting O8 III stars in the central $1''\!.5$ of the Galaxy show that their winds result in an absorbed luminosity of 2.4×10^{32} erg s^{-1}. Although the simulated spectrum is harder than that observed, it appears that at least 10% of the *Chandra* point source is due to emission from fairly far away from the putative black hole's event horizon. However, if there are more O stars in the central milliparsecs or if their winds are stronger, there will be even more extended emission. Also, a significant portion of the winds from stars further out is likely to be trapped in the central $0''\!.1$ (Coker & Melia, 1997). Therefore, it is quite possible that all of the *Chandra* point source is in fact extended emission on the scale of $\sim 0.1''$. This would imply that only the flared emission is coming from near the black hole event horizon. As a result, accretion models for Sgr A* which predict constant significant X-ray emission from near the black hole may need to be revised.

Acknowledgments

This work was performed under the auspices of the US Department of Energy by the Los Alamos National Laboratory under contract W-7405-ENG-36. JMP would like to thank PPARC UK for the funding of a PDRA position. This research has made use of NASA's Astrophysics Data System Abstract Service.

References

Aschenbach, B., Grosso, N., Porquet, D., Predehl, P. 2004, A&A, 417, 71

Baganoff, F. K., et al. 2001, Nature, 413, 45

Baganoff, F. K., et al. 2003, ApJ, 591, 891

Baltrusaitis, R. M., et al. 1996, Physics of Fluids, 8, 2471

Coker, R. F., Melia, F. 1997, ApJ, 488, L149

Falcke, H., Körding, E., Markoff, S. 2004, A&A, 414, 895

Ferland, G. J. 2000, Revista Mexicana de Astronomia y Astrofisica Conference Series, 9, 153

Garmany, C. D., Conti, P. S. 1984, ApJ, 284, 70

Figure 6: A synthetic image (with red=2–3 keV, green=3–5 keV, and blue=5–10 keV) of the X-ray emission from the gas distribution shown in Fig. 4. Sgr A* dominates the emission although some of the individual stars can still be seen.

Geballe, T. R., Krisciunas, K., Bailey, J. A., Wade, R. 1991, ApJ, 370, L73

Ghez, A. M., et al. 2004, ApJ, submitted (astro-ph/0306130)

Krtička, J., Kubát, J. 2004, A&A, 417, 1003

Melia, F., Falcke, H. 2001, ARA&A, 39, 309

Mewe, R., Gronenschild, E. H. B. M., van den Oord, G. H. J. 1985, A&AS, 62, 197

Pittard, J. M., Stevens, I. R. 1997, MNRAS, 292, 298

Rockefeller, G., Fryer, C. L., Melia, F., Warren, M. S. 2004, ApJ, 604, 662

Strickland, D. K., Stevens, I. R. 1998, MNRAS, 297, 747

Weinberg, N. N., Milosavljevic, M., Ghez, A. M. 2004, ApJ, submitted (astro-ph/0404407)

Yuan, F., Markoff, S., Falcke, H. 2002, A&A, 383, 854

Yuan, F., Quataert, E., Narayan, R. 2003, ApJ, 598, 301